Coating Single-Walled Carbon Nanotubes with Tin Oxide

Wei-Qiang Han and A. Zettl*

Department of Physics, University of California at Berkeley, and Material Sciences Division, Lawrence Berkeley National Laboratory, Berkeley, California 94720

Received March 9, 2003; Revised Manuscript Received March 20, 2003

ABSTRACT

Single-walled carbon nanotubes coated with crystalline tin oxide by a simple chemical-solution route are reported. The room-temperature chemical treatment results in a nominally complete and uniform coating over the entire outer surface of singular nanotubes, nanotube bundles, and also fullerene-like nanoparticles. The samples have been characterized by high-resolution transmission electron microscopy, energy-dispersive X-ray spectrometry, and X-ray diffraction. The coating is composed of interconnected SnO_2 nanoparticles of sizes between 1–6 nm. Typically, the coatings have a total thickness on the order of the constituent nanoparticle size.

The atomically well-defined 1D structure of single-walled carbon nanotubes (SWCNTs) provides a new model system for basic scientific studies and pathways to nanoscale devices.[1] The physical properties of SWCNTs can be dramatically influenced by surface modification with selected organic, inorganic, and biological species.[2-8] Such functionalization can lead to a significant enhancement of properties that are relevant to technological applications. Recently, it has been demonstrated that SWCNTs and SWCNTs functionalized with ultrathin coatings represent a new type of chemical sensor capable of detecting small concentrations of molecules under ambient conditions.[5,9,10] For decoration by inorganic species, SWCNTs have been coated with various metal nanoparticles such as Au, Ti, Ni, Pd, Al, Fe, Pb, and Pt by electron-beam evaporation or electroless metal deposition.[2,5,11] Single amine-functionalized CdSe nanoparticles were coupled to SWCNTs via amide bond formation.[12] Recently, Fu et al. reported coating SWCNTs with a thin SiO_2 layer using 3-aminopropyltriethoxyysilane as coupling layers.[13]

SnO_2 is an n-type semiconductor with a wide energy gap. It plays a key role in applications such as conductive electrodes, transparent coatings, heterojunction solar cells, and chemical sensors. The deposition techniques used for SnO_2-based films include chemical vapor deposition, sol−gel, paste/slurry deposition, sputtering, and evaporation.[14,15]

Chemical routes for deposition involve using metal salts as precursors. SnO_2 films can be prepared by the gas-phase reaction of $SnCl_4$ with H_2O[16] or by the gas-phase reaction of $SnCl_4$ with O_2.[17] $SnCl_4 \cdot 5H_2O$ has been used to prepare SnO_2 particle films with particles of size 24−33 nm via a pyrolysis method.[18] From a technological viewpoint, two extremes in the preparation of SnO_2-based sensors appear to be successful: thick films with controlled nanocrystalline sizes and thin films with monolayers of nanocrystalline SnO_2.[19] Recently, Comini et al. reported SnO_2 nanobelts (width ∼200 nm) that are sensitive to CO, NO, and ethanol.[20]

Here we report a simple and efficient room-temperature chemical route using $SnCl_2$ as a precursor to coat SWCNTs fully with a thin, nominally uniform layer of SnO_2. This work is motivated by potential applications of the combined $SWCNT/SnO_2$ system.

Commercially available SWCNTs of Tubes@Rice are used in this work. These SWCNTs are produced by a laser ablation method using nickel as a catalyst. The nanotubes are high quality and quite pure, although some fullerene-like nanoparticles (FNPs) still exist in the purchased material as a byproduct. SWCNTs are formed either as isolated units or as nanotubes arranged in bundles; no attempt was made to separate the different configurations. SWCNTs were first treated with nitric acid (40%) inside a glass flask at 120 °C for 1 h to clean the nanotubes' surfaces. The treated SWCNTs were then rinsed with distilled H_2O. One gram of tin(II) chloride (anhydrous, Alfa, 99%) was put into 40 mL of distilled H_2O inside a glass flask , and then 0.7 mL of HCl (38%) was added. We then immersed 10 mg of the acid-treated SWCNTs in the above solution. This solution was sonicated for 3−5 min and then stirred for 45−60 min at room temperature. The treated nanotube sample was then rinsed with distilled H_2O. Both the template SWCNTs and SWCNTs coated with SnO_2 solutions are treated through filtering. The samples were finally characterized using X-ray diffraction (XRD) with Cu Kα radiation and high-resolution transmission electron microscopy (HRTEM) using a JEOL JEM-2010 and Philips CM200 FEG equipped with an
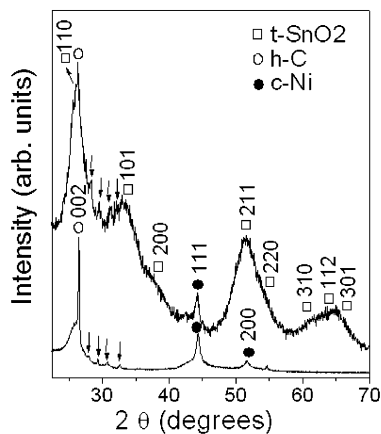
Figure 1. XRD spectrum of the product (upper curve) is identified as tetragonal SnO_2. Hexagonal C, cubic Ni, and other small diffraction peaks (labeled by arrows) come from the template SWCNTs. The XRD spectrum of the SWCNTs before coating (lower curve) shows the same template diffraction peaks.

energy-dispersive X-ray spectrometer (EDS). For TEM analysis, the material was ultrasonically dispersed in 2-propanol and dropped onto a holey-carbon-coated copper grid.

Figure 1 shows XRD patterns of the specimen (upper curve) and template SWCNTs (lower curve). The XRD spectrum taken from the uncoated SWCNTs indicates that the maximal peak is composed of a sharp peak superimposed onto a weak broad peak. Both peaks come from hexagonal carbon (002) (JCPDS 26-1079). Any signature XRD peaks of hexagonal graphite do not come from pure SWCNTs.[21] Checking with TEM, we find that the sharp peak comes from graphite particles from the laser ablation target. The broad peak comes from some FNPs, onions, and a small amount of multiwalled CNTs. Two cubic nickel (*c*-Ni) peaks (111) and (200) (JCPDS 04-0850), which originate from the remnant Ni catalyst, are observed. Some unclear small peaks are also observed. The maximal diffraction peaks of the specimen (upper curve) are consistent with the known tetragonal SnO_2 (*t*-SnO_2) lattice constants given in the literature as $a = 4.755$ Å and $c = 3.199$ Å (JCPDS 41-1445). The main peak of tetragonal $SnO_2(110)$ almost overlaps with the main peaks of *h*-C(002). Comparing both spectra, it is easy to find that the broad peak is mainly contributed from SnO_2. The Ni peak and other unclear peaks come from the impurities of used SWCNTs. No obvious peaks corresponding to $SnCl_2$, Sn, or other tin oxides are observed in the powder pattern.

Figure 2a shows a typical low-resolution TEM image of the specimen. The SWCNTs usually appear as bundles with some appearing as individuals. We observe that almost all nanotubes or nanotubes bundles in the sample have been fully coated with thin and uniform layers. The thickness of the coating is usually less than 5 nm. FNPs in the sample have also been fully and uniformly coated. Figure 2b shows a high-resolution TEM image of a fully coated SWCNT. The coating is rather uniform, with an average thickness of about 4 nm. The coating layer is composed of SnO_2 nanoparticles with sizes of less than 6 nm. The broad peaks of SnO_2 in the XRD spectrum (Figure 1) are consistent with the
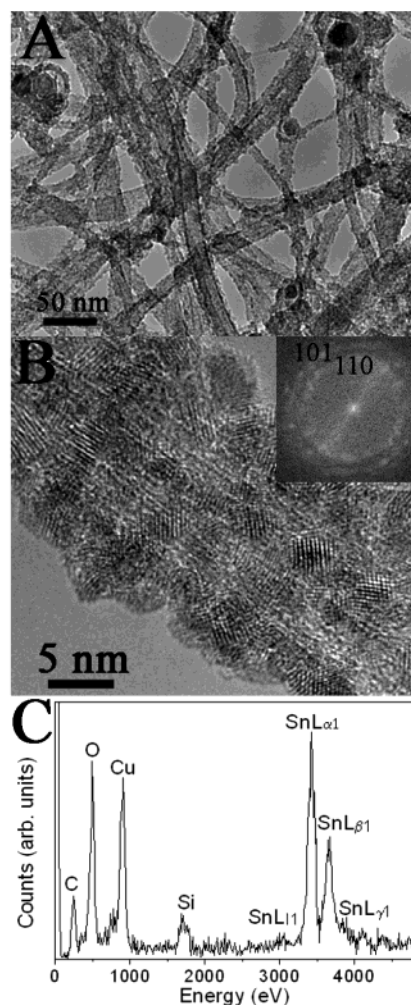

Figure 2. (A) Low-resolution TEM image of fully coated SWCNTs. (B) High-resolution TEM image of a SWCNT bundle fully coated with SnO_2. The inset is the corresponding FFT diffraction pattern. The three polycrystalline rings correspond to crystal faces of (110), (101), and (200) of tetragonal SnO_2. (C) Typical EDS spectrum of SnO_2-coated SWCNTs. The atomic ratio of O to Sn is near 2.

nanoparticles being small. The average size of nanoparticles calculated by the Scherrer equation is about 4 nm, which is consistent with the TEM results. Measurements of lattice fringe spacing of nanoparticles show contributions mainly from (110) and (101) planes of *t*-SnO_2. Fast Fourier transform (FFT) analysis of selected regions of the coating reveals details of the local SnO_2 structure. The inset to Figure 2b is the corresponding FFT diffraction pattern, which can be indexed to tetragonal SnO_2. The two clear polycrystalline rings correspond to crystal faces of (110) and (101) of *t*-SnO_2, which is in accordance with the above measurement results of lattice fringe spacing. Chemical analysis using EDS indicates the presence of Sn, O, and C in the coated SWCNTs, nanotube bundles, and FNPs. The C signal originates from the supporting SWCNTs. For the majority of the coated nanotubes and coated nanotube bundles, the atomic ratio of O to Sn is close to 2 (Figure 2c). The atomic ratio of O to Sn was calculated by the standard procedure of ES Vision software. Commercially available SnO_2 powder (Alfa) was used for calibration. The small Si peak in Figure
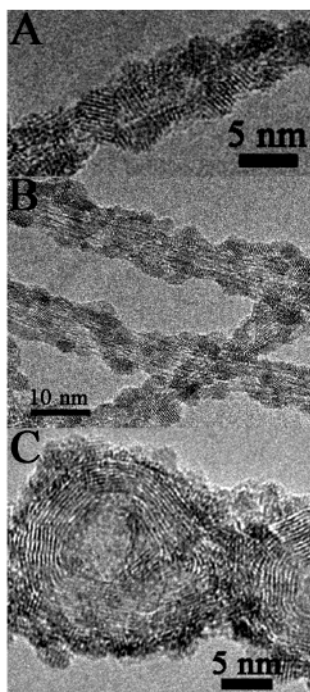
Figure 3. (A) High-resolution TEM image of an individual SWCNT fully coated with SnO_2. (B) High-resolution TEM image of three small SWCNT bundles fully coated with SnO_2. (C) High-resolution TEM image of two FNPs fully coated with SnO_2.

2c may come from contamination of the glass flask reacting with nitric acid during the pretreatment of SWCNTs. The Si peak might also come from the quartz-tube laser-ablation chamber. The Cu signal comes from the copper grid. For a small number of nanotubes, the coatings indicated O to Sn ratios between 1 and 2.

Figure 3a is a high-resolution TEM image of an individual SWCNT fully coated with SnO_2. The coating of the individual SWCNT is uniform and thin, with an average thickness of 3 nm. Here, the coating layer is composed of SnO_2 nanoparticles whose sizes are less than 5 nm. Figure 3b shows three small SWCNT bundles fully coated with SnO_2. The coating is uniform, with an average thickness of about 3 nm. The coating layer is composed of nanoparticles with sizes of less than 6 nm. Figure 3c shows two FNPs fully coated with SnO_2. The coating again is uniform, with an average thickness of about 3 nm. The coating layer is composed of SnO_2 nanoparticles with sizes of less than 5 nm. The SnO_2 coating layer of the filled FNP follows the shape of the supporting FNP template.

The high-resolution TEM, EDS, and XRD results reveal that the consistent and uniform nanometer-scale SnO_2 coverage is independent of the precise morphology of the SWCNTs and C nanoparticles. In this case, the chemical reaction leading to SnO_2 is unclear. Two possibilities are described by the following chemical reactions:

$$2SnCl_2 + 2H_2O + O_2 \rightarrow 2SnO_2 + 4HCl \qquad (1)$$

$$SnCl_2 + 2H_2O \rightarrow SnO_2 + 2HCl + H_2 \qquad (2)$$
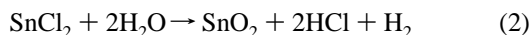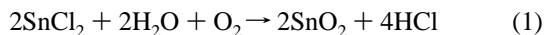
Since the observed reaction does not produce gas (i.e., bubbles), the first reaction is more probable.

We now briefly discuss possible applications of these compound materials. It is believed that sensor sensitivity can be improved by increasing the specific surface area of the active materials. One direct way to increase the specific surface area is to decrease the size of the particles of the active material. A SnO_2 thin film composed of nanoparticles with mean sizes between 3 and 15 nm has shown high gas sensitivity and improved gas selectivity in comparison to sensors consisting of micrometer-sized grains.[22] In the present work, we have observed the formation of thin, uniform, and uninterrupted coverage SnO_2 nanoparticles on single-walled carbon nanotubes. SnO_2 and SWCNTs are both well known as active components in molecular detection and transudation systems, suggesting nanoscale sensor applications for these functionalized SWCNTs. The possible formation of Sn−C bonds on the interface of ultra-fine nanoparticles of SnO_2 and nanotubes might change the localized electron system. We anticipate that the SnO_2 thin coating with ultra-fine SnO_2 nanoparticles produced in the present work might also exhibit other interesting physical properties relevant to potential applications.

References

(1) Iijima, S.; Ichihashi, T. *Nature (London)* **1993**, *363*, 603.
(2) Zhang, Y.; Franklin, N.; Chen, R.; Dai, H. *Chem. Phys. Lett.* **2000**, *331*, 35.
(3) Chen, R.; Zgang, Y.; Wang, D.; Dai, H. *J. Am. Chem. Soc.* **2001**, *123*, 3838.
(4) Erlanger, B.; Chen, B.; Zhu, M.; Brus, L. *Nano Lett.* **2001**, *1*, 465.
(5) Kong, J.; Chapline, M.; Dai, H. *Adv. Mater.* **2001**, *13*, 1384.
(6) Baker, S.; Cai, W.; Lasseter, T.; Weidkamp, K.; Hamers, R. *Nano Lett.* **2002**, *2*, 1413.
(7) Azamian, B.; Davis, J.; Coleman, K.; Bagshaw, C.; Green, M. L. H. *J. Am. Chem. Soc.* **2002**, *124*, 12664.
(8) Georgakilas, V.; Kordatos, K.; Prato, M.; Guldi, D.; Holzinger, M.; Hirsch, A. *J. Am. Chem. Soc.* **2002**, *124*, 760.
(9) Collins, P.; Bradley, K.; Ishigami, M.; Zettl, A. *Science (Washington, D.C.)* **2000**, *287*, 1801.
(10) Kong, J.; Franklin, N.; Zhou, C.; Chapline, M.; Peng, S.; Cho, K.; Dai, H. *Science (Washington, D.C.)* **2000**, *287*, 622.
(11) Choi, H.; Shim, M.; Bangsaruntip, S.; Dai, H. *J. Am. Chem. Soc.* **2002**, *124*, 9058.
(12) Haremza, J.; Hahn, M.; Krauss, T.; Chen, S.; Calcines, J. *Nano Lett.* **2002**, *2*, 1253.
(13) Fu, Q.; Lu, C.; Liu, J. *Nano Lett.* **2002**, *2*, 329.
(14) Kohl, D. *J. Phys. D: Appl. Phys.* **2001**, *34*, R125.
(15) Simon, I.; Barsan, N.; Bauer, M.; Weimar, U. *Sens. Actuators, B* **2001**, *73*, 1.
(16) Aboaf, A.; Marcotte, V.; Chou, N. *Electrochem. Soc.* **1973**, *120*, 701.
(17) Nagano, M. *J. Cryst. Growth* **1984**, *67*, 639.
(18) Maudes, J.; Rodriquez, T. *Thin Solid Films* **1980**, *69*, 183.
(19) Barsan, N.; Schweizer-Berberich, M.; Gopel, W. *Fresenius' J. Anal. Chem.* **1999**, *365*, 287.
(20) Comini, E.; Faglia, G.; Sberveglieri, G.; Pan, Z.; Wang, Z. *Appl. Phys. Lett.* **2002**, *81*, 1869.
(21) Rols, S.; Almairac, L.; Henrard, L.; Anglaret, E.; Sauvajol, J. L. *Eur. Phys. J. B* **1999**, *10*, 270.
(22) Ogawa, H.; Nishikawa, M.; Abe, A. *J. Appl. Phys.* **1982**, *53*, 4448.